Experimental Gerontology 47 (2012) 100–108

Contents lists available at SciVerse ScienceDirect

Experimental Gerontology

journal homepage: www.elsevier.com/locate/expgero

Long-term perturbation of muscle iron homeostasis following hindlimb suspension in old rats is associated with high levels of oxidative stress and impaired recovery from atrophy

Jinze Xu [a,*,1], Judy C.Y. Hwang [a,1], Hazel A. Lees [a], Stephanie E. Wohlgemuth [a], Mitchell D. Knutson [b], Andrew R. Judge [c], Esther E. Dupont-Versteegden [d], Emanuele Marzetti [a,e], Christiaan Leeuwenburgh [a,**,1]

[a] Department of Aging and Geriatric Research, Division of Biology of Aging, Genomics and Biomarkers Core of The Institute on Aging, University of Florida, Gainesville, Florida, USA
[b] Food Science and Human Nutrition Department, University of Florida, Gainesville, USA
[c] Department of Physical Therapy, University of Florida, Gainesville, USA
[d] Department of Rehabilitation Sciences, Division of Physical Therapy, University of Kentucky, Lexington, USA
[e] Department of Orthopaedics and Traumatology, Catholic University of the Sacred Heart, Rome, Italy

ARTICLE INFO

Article history:
Received 14 April 2011
Received in revised form 6 October 2011
Accepted 28 October 2011
Available online 4 November 2011

Section Editor: Andrzej Bartke

Keywords:
Aging
Sarcopenia
Iron metabolism
Hindlimb unloading and re-loading
Skeletal muscle atrophy

ABSTRACT

In the present study, we investigated the effects of 7 and 14 days of re-loading following 14-day muscle unweighting (hindlimb suspension, HS) on iron transport, non-heme iron levels and oxidative damage in the gastrocnemius muscle of young (6 months) and old (32 months) male Fischer 344×Brown Norway rats. Our results demonstrated that old rats had lower muscle mass, higher levels of total non-heme iron and oxidative damage in skeletal muscle in comparison with young rats. Non-heme iron concentrations and total non-heme iron amounts were 3.4- and 2.3-fold higher in aged rats as compared with their young counterparts, respectively. Seven and 14 days of re-loading was associated with higher muscle weights in young animals as compared with age-matched HS rats, but there was no difference in muscle weights among aged HS, 7 and 14 days of re-loading rats, indicating that aged rats may have a lower adaptability to muscle disuse and a lower capacity to recover from muscle atrophy. Protein levels of cellular iron transporters, such as divalent metal transport-1 (DMT1), transferrin receptor-1 (TfR1), Zip14, and ferroportin (FPN), and their mRNA abundance were determined. TfR1 protein and mRNA levels were significantly lower in aged muscle. Seven and 14 days of re-loading were associated with higher TfR1 mRNA and protein levels in young animals in comparison with their age-matched HS counterparts, but there was no difference between cohorts in aged animals, suggesting adaptive responses in the old to cope with iron deregulation. The extremely low expression of FPN in skeletal muscle might lead to inefficient iron export in the presence of iron overload and play a critical role in age-related iron accumulation in skeletal muscle. Moreover, oxidative stress was much greater in the muscles of the older animals measured as 4-hydroxy-2-nonhenal (HNE)-modified proteins and 8-oxo-7,8-dihydroguanosine levels. These markers remained fairly constant with either HS or re-loading in young rats. In old rats, HNE-modified proteins and 8-oxo-7,8-dihydroguanosine levels were markedly higher in HS and were lower after 7 days of recovery. However, no difference was observed following 14 days of recovery between control and re-loading animals. In conclusion, advanced age is associated with disruption of muscle iron metabolism which is further perturbed by disuse and persists over a longer time period.

Published by Elsevier Inc.

1. Introduction

Acute muscle atrophy induced by unloading is accompanied by profound morphological and biochemical alterations, the recovery from which is impaired at advanced age (Zarzhevsky et al., 2001). Disruption of muscle iron homeostasis has recently emerged as a potential factor involved in the pathogenesis of both sarcopenia of aging and disuse-induced muscle atrophy (Xu et al., 2010a). Indeed, acute atrophy following hindlimb suspension (HS) is associated with markedly higher iron levels in skeletal muscle in aged rodents

* Correspondence to: J. Xu, Division of Biology of Aging, Department of Aging and Geriatrics, College of Medicine, University of Florida, Institute on Aging, USA. Tel.: +1 352 273 5726.
** Correspondence to: C. Leeuwenburgh, Department of Aging and Geriatric Research, Institute on Aging, Division of Biology of Aging, University of Florida, PO Box 112610, Gainesville, FL 32611, USA. Tel.: +1 352 273 6796; fax: +1 352 273 5920.
E-mail addresses: jxu@aging.ufl.edu (J. Xu), cleeuwen@aging.ufl.edu (C. Leeuwenburgh).
[1] These authors contributed equally to this work.

0531-5565/$ – see front matter. Published by Elsevier Inc.
doi:10.1016/j.exger.2011.10.011

in conjunction with extensive oxidative damage (Hofer et al., 2008b). Although essential for several life sustaining functions, iron is a highly redox-active metal capable of converting oxidant intermediates, such as hydrogen peroxide, into harmful free radical species (e.g., hydroxyl radical). Nucleic acids are good chelators of metals, making them especially vulnerable to iron-mediated damage in the presence of reactive oxygen species (ROS) (Wacker and Vallee, 1959). Moreover, iron can catalyze the nitration of tyrosine residues resulting in extensive protein damage (Bian et al., 2003). Hence, excessive iron accumulation may lead to considerable damage to muscle constituents, thereby contributing to the development of atrophy.

Iron is found in two main forms in the body: heme iron and non-heme iron. Iron as a part of heme is very stable. Non-heme iron occurs in several forms: stored in either the cytosolic protein ferritin or in the hemosiderin complex, as iron-sulfur clusters in enzymes of the electron transport chain, or as atomic iron bound to enzymes or as part of the transport protein transferrin (Hider and Zhou, 2005; Lill and Muhlenhoff, 2006). A distinct fraction of chelatable non-heme iron is referred to as the labile-iron pool, which is extremely reactive and can produce highly destructive hydroxyl radicals even at trace levels (Xu et al., 2010a). The age-related accumulation of non-heme iron in tissues increases the availability of labile redox-active iron, which may be causal to the extensive amounts of oxidative damage to biomolecules observed in aged tissue.

Cellular uptake, storage, transport and export of iron are tightly regulated through a multitude of factors (Chua et al., 2007; Dunn et al., 2007; Kohgo et al., 2008). Iron cannot diffuse through cellular membranes unassisted. The primary route of cellular iron acquisition is through receptor-mediated endocytosis of transferrin (Tf) (Leverence et al., 2010). Cells take up Tf-bound iron in proportion to their cell-surface expression of transferrin receptor (TfR1) (Hofer et al., 2008a). During states of iron overload, a non-Tf-bound iron uptake pathway mediated by divalent metal transporter-1 (DMT1), Zip14 or L-type voltage-dependent Ca^{2+} channels (LVDCCs) may occur. DMT1 can import iron into the cell, a mechanism which is essential for intestinal uptake of inorganic sources of dietary iron (Dunn et al., 2007). Zip14 is a member of the SLC39A zinc transporter family, which is also involved in iron uptake by cells (Liuzzi et al., 2006). In addition to playing a role in the non-Tf bound uptake pathway, DMT1 and Zip14 also participate in the assimilation of iron from Tf, suggesting that they are involved in both pathways of iron acquisition (Zhao et al., 2010; Xu et al., 2010a). Iron export is mediated by ferroportin (FPN), the only known iron exporter in mammals to date (Donovan et al., 2005).

Although numerous studies have investigated cellular iron metabolism, little work has been conducted to investigate the effects of age, loading and re-loading on muscle iron transport. The present study was designed to examine age-related changes in iron homeostasis in rats subjected to muscle unloading and subsequent reloading. We hypothesized that the expression levels of myocyte iron transport proteins in aged animals would be altered during the development of acute muscle atrophy and would persist after HS, in conjunction with elevated levels of oxidative damage and impaired recovery from atrophy.

2. Materials and methods

2.1. Animals and experimental procedures

The study was approved by the Institutional Animal Care and Use Committee at the University of Kentucky. All procedures were performed in accordance with the National Institutes of Health guidelines for the care and use of laboratory animals. Male Fischer 344×Brown Norway rats (6 and 32 months of age) were purchased from the National Institute on Aging. Rats were divided into four groups (n=8/each): non-suspended control, 14 days of HS, 14 days of HS followed by 7 days of ambulatory re-loading (HS+7), and 14 days of HS followed by 14 days of ambulatory re-loading (HS+14). Animals were individually housed and maintained on a 12-h light/dark cycle, at constant temperature and humidity, in a facility approved by the Association for Assessment and Accreditation of Laboratory Animal Care. Rats had free access to NIH-31 average nutrient composition pellets and tap water. HS was performed as described previously (Gallegly et al., 2004; Hofer et al., 2008b). Briefly, a tail device containing a hook was attached with gauze and cyanoacrylate glue while the animals were anesthetized with isoflurane (5% induction, 2% maintenance). After the animal regained consciousness, the tail device was connected via a thin cable to a pulley sliding on a vertically adjustable stainless steel bar running longitudinally above a high-sided cage. The system was designed in such a way that the rats could not rest their hind limbs against any side of the cage. Finally, rats were euthanized with an overdose of sodium pentobarbital (100 mg/kg). Gastrocnemius muscles were dissected, weighed, frozen in liquid nitrogen, and stored at −80 °C until analysis. Muscle weights are reported as the average between the two legs. The gastrocnemius was selected for the study due to its mixed fiber composition, thus allowing for generalizing the results to other muscles. In addition, the substantial amount of tissue in gastrocnemius muscle allowed us to perform all the analyses on the same muscle.

2.2. Non-heme iron levels in the gastrocnemius muscle of rats

Muscle levels of non-heme iron were measured as previously described (Rebouche et al., 2004; Hofer et al., 2008b). Briefly, ~50 mg of the left gastrocnemius muscle was trimmed of fat and tendons and homogenized in deionized water (1:10 w:v) using a glass-glass Duall homogenizer on slush ice. A commercially available iron standard (High-Purity Standards, Charleston, SC) was diluted to 2, 4, 6, 8, and 10 μg iron/ml in deionized water. An equal amount of protein precipitation buffer [1 N HCl and 10% (v/v) trichloroacetic acid] was added to an aliquot (80 μl) of the homogenates, a blank (deionized water), or the iron standards, and the samples were incubated at 95 °C for 60 min to denature proteins. Following centrifugation at 10,000×*g* for 10 min, the supernatant was collected and divided into two fractions. An equal amount of sample blank solution (1.5 M sodium acetate and 0.1% thioglycolic acid) was added to 40 μl of the supernatant, and a chromogen solution (0.508 mM ferrozine, 1.5 M sodium acetate, and 0.1% thioglycolic acid) was added to 70 μl of the supernatant. After 30 min of color development at room temperature, the absorption was determined at 562 nm in a quartz cuvette using a Beckman DU 640 spectrophotometer. After correction from sample blanks, the iron concentration was calibrated against the iron standard curve and expressed as μg per g of muscle.

2.3. Western blot analysis

Whole-tissue extracts were prepared by homogenization of frozen gastrocnemius muscle (~100 mg) using a polytron in HEM buffer (20 mM HEPES, 1 mM EDTA, 300 mM mannitol, pH 7.0) containing a cocktail of protease inhibitors (Sigma, St Louis). For the preparation of a membrane-enriched fraction, insoluble debris in tissue lysates were removed by low-speed centrifugation (10,000×*g*, 10 min, 0 °C). The membrane fraction was pelleted by centrifugation at 100,000×*g* for 30 min and membranes resuspended in HEM buffer. After determination of protein concentration by the Bradford assay (Bradford, 1976), membrane proteins were applied to pre-cast Tris·HCl gels (Bio-Rad, Hercules, CA) and transferred onto polyvinylidene difloride (PVDF) (Millipore) or nitrocellulose (BioRad) membranes. For FPN detection, samples were free of β-mercaptoethanol and non-boiled before loading. Blots were blocked in StartingBlock Blocking Buffer in Tris-buffered saline (TBS, pH 7.5) with 0.05% Tween 20 (TBS-t, Pierce Biotechnology, Rockford, IL) for 60 min at

room temperature and probed with primary antibodies against TfR1 (Zymed, San Francisco, CA; dilution 1:2,000), FPN (1:200) (Knutson et al., 2005; Hansen et al., 2010; Xu et al., 2010b), DMT1 (courtesy of Dr. Philippe Gros, McGill University; dilution 1:2,500), hemojuvelin (HJV) (courtesy of Dr. An-Sheng Zhang, Oregon Health and Science University; dilution 1:400) (Zhang et al., 2010), Zip14 (1:100) (Knutson et al., 2005). Secondary antibody incubation was carried out for 30 min at room temperature, using anti-mouse (Sigma-Aldrich; 1:30,000) and anti-goat (Santa Cruz Biotechnology; 1:5,000) alkaline phosphatase-conjugated secondary antibodies. Membranes were washed in TBS-t, rinsed in TBS, and washed in Tris·HCl (100 mM, pH 9.5). Finally, the chemiluminescent substrate for alkaline phosphatase (Vector Laboratories, Burlingame, CA) was applied and the chemiluminescent signal captured with an Alpha Innotech Fluorchem SP imager (Alpha Innotech, San Leandro, CA). Digital images were analyzed using the AlphaEase FC software (Alpha Innotech). Spot density of target bands was normalized to the amount of protein loaded in each lane, as determined by densitometric analysis of the corresponding Ponceau S-stained membranes (Marzetti et al., 2009) and expressed as arbitrary optical density (OD) units.

2.4. Quantitative real-time polymerase chain reaction (qRT-PCR)

To determine the relative gene expression of iron-related proteins, qRT-PCR analysis was performed. Total RNA was isolated and DNase-treated as previously described (Marzetti et al., 2008a). First strand cDNA synthesis was achieved from 2 μg of RNA using the MasterScript kit (5 Prime, Hamburg, Germany). qRT-PCR was performed using an Applied Biosystems 7300 Real-Time PCR System (ABI, Foster City, CA). Primers were designed with the on-board software Primer Express 3.0 (Table 1). Power SYBR Green PCR Master Mix (ABI) was used employing ABI universal cycling conditions. Analysis of dissociation curves revealed single product amplifications. All samples were examined in triplicate, with the young non-suspension control group as a calibrator. For all genes, negative controls (i.e., no template and no reverse transcriptase) were also included. Differences in the expression of the target genes were determined by the $2^{-\Delta\Delta CT}$ method (Livak and Schmittgen, 2001) with β-actin as the housekeeping gene, the expression of which did not differ among the experimental groups.

2.5. Dot blot analysis for 3-nitrotyrosine and HNE

HNE-adducts and 3-nitrotyrosine were determined via dot blot analysis as previously described (Marzetti et al., 2008b). Briefly, 3 and 5 μl of gastrocnemius homogenate for 3-nitrotyrosine and HNE-adducts were loaded onto a nitrocellulose membrane (Bio-Rad), respectively. Membranes were air-dried for 20 min and blocked in 2% casein with 0.05% Tween 20 for 1 h at room temperature. Membranes were subsequently incubated in primary antibody for 30 min at room temperature and washed three times in TBS-t (Pierce Biotechnology). The following primary antibodies and relative dilutions were used: mouse monoclonal anti-3-nitrotyrosine (Santa Cruz Biotechnology, Biotechnology, Santa Cruz, CA, 1:200); goat polyclonal anti-HNE (Alpha Diagnostic, San Antonio, TX, 1:500). Secondary antibody incubation was carried out for 30 min at room temperature, using anti-mouse (Sigma-Aldrich, 1:30,000) and anti-goat (Santa Cruz Biotechnology, 1:5,000) alkaline phosphatase-conjugated secondary antibodies. Membranes were washed in TBS-t, TBS, and Tris·HCl (100 mM, pH 9.5). Generation of the chemiluminescent signal, digital acquisition and densitometry analysis were performed as described in the Western blot experiments. Density of the target spot was normalized to total protein concentration as determined by the detergent-compatible D_C assay (Bio-Rad) and expressed as arbitrary OD units % of total protein.

Table 1
Summary of primer sequences of the investigated genes.

	Forward primer	Reverse primer
TfR1	GAATACGTTCCCCGTTGTTGA	ATCCCCAGTTCCTAGATGAGCAT
DMT1 IRE	TGTGGCCTGGCGTTACG	CGCAGAAGAACGAGGACCAA
DMT1 nonIRE	TTTGAACCAAGGCGAAGAAGA	ACCCATTCACAGCCGTTAGC
Zip14	CCTCACGAGCTGGGAGACTTC	AGAGGGCCTGCTGGATACTCA
HJV	GGGAGCCACGTGGAGATTC	GCTGTCTGACGAACGATTATAGTT
FPN	GGTGGTGGCAGGCTCTGT	TTTGAACCACCAGGGACGTC

2.6. Measurement of RNA and DNA oxidation using HPLC-ECD

Oxidation of RNA and DNA was quantified using a high-performance liquid chromatography coupled with electrochemical detection (HPLC-ECD) method as 8-oxo-7,8-dihydroguanosine/10^6 guanosine and 8-oxo-7,8-2′-deoxyguanosine/10^6 deoxyguanosine, respectively (Hofer et al., 2006, 2008b; Xu et al., 2008). This procedure is based on high-salt nucleic acid release from proteins, followed by removal of proteins and fats by organic solvents at neutral pH, all in the presence of the metal chelator deferoxamine mesylate (DFOM) at 0 °C. Muscle pieces were thawed, stripped of tendons on ice, weighed (~100 mg), minced, and homogenized on slush ice using a glass-glass Duall homogenizer in 2 ml (1:10 w:v) 3 M guanidine thiocyanate (GTC) buffer [0.2% (w/v) N-lauroylsarcosinate, 20 mM Tris, pH 7.5] containing 10 mM freshly prepared DFOM. After transferring the solution into phase-lock gel (PLG) tubes, an equal volume of phenol/chloroform/isoamyl alcohol (25:24:1, pH 6.7) was added and the samples were immediately vortexed, followed by a 10 min vortexing period at 0 °C to completely release nucleic acids as previously described (Hofer et al., 2006). After centrifugation (14,000×*g*, 10 min, 0 °C), the aqueous phase was transferred into a new PLG tube and extracted with an equal volume of chloroform/isoamyl alcohol (24:1). Samples were hand-shaken and centrifuged, and the aqueous phase was collected followed by nucleic acid precipitation at −80 °C overnight after the addition of an equal amount of isopropanol. After centrifugation (14,000×*g*, 10 min, 0 °C), nucleic acids were washed with 70% (v/v) ethanol, dried, dissolved in 100 μl DNAse and RNase-free water containing 30 μM DFOM, and hydrolyzed using 4 U nuclease P_1 and 5 U alkaline phosphatase in buffer (30 mM sodium acetate, 20 μM $ZnCl_2$, pH 5.3) at 50 °C for 60 min. After filtration, samples were analyzed by high-performance liquid chromatography coupled to electrochemical and UV detection (HPLC-ECD/UV).

2.7. Statistical analysis

Statistical analyses were performed using GraphPad Prism Version 4.0 (GraphPad Software, San Diego, CA). The experiments were fully crossed, two-factor designs, with 2 levels of age (6 and 32 months) and 4 levels of treatment (Control, HS, HS + 7 and HS + 14). The two-way analysis of variance (ANOVA) allowed for the distinction between age and treatment effects as well as for the determination of a possible interaction between the two factors. We also reported whether there was a main age effect (independent of treatment) and/or a main effect of treatments (independent of age). When applicable, Tukey's multiple comparison test was performed. All tests were two-sided with significance set at $p<0.05$. All data are reported as mean ± SEM. Correlations between variables were explored using Pearson's test. All tests were two-sided with statistical significance defined as $p<0.05$. Data are presented as mean ± SEM.

3. Results

3.1. Advanced age and HS were associated with muscle atrophy

Body weight (BW) was higher in old animals than their young counterparts. HS and re-loading were associated with lower BW in

both young and aged animals as compared with their age-matched controls (age effect: $p<0.0001$; treatment effect: $p<0.0001$; age × treatment interaction: $p<0.05$; Table 2). Muscle weight (MW) and MW to BW ratio (MW/BW) were lower in old controls than young rats (age effect: $p<0.0001$; Table 2). HS was associated with lower MW and MW/BW in both young and old cohorts (treatment effect: $p<0.0001$; Table 2). Difference in MW between HS and re-loading was observed in 6-month-old rats (age × treatment interaction: $p<0.05$), but not in 32-month-old rats. Young animals subjected to 14 days of re-loading had higher MW than their age-matched rats subjected to 7 days of re-loading. In contrast, there was no difference in MW and MW/BW between HS, 7 days and 14 days of re-loading in old rats.

3.2. HS and re-loading were associated with higher non-heme iron concentrations in the gastrocnemius muscle of old, but not young rats

Non-heme iron concentrations in the gastrocnemius muscle of rats were 3.4-fold higher in 32-month-old controls as compared with their young counterparts (age effect: $p<0.0001$; Fig. 1A). Fourteen days of HS was associated with a much higher concentration of non-heme iron in muscles of old rats ($p<0.05$), whereas no difference was observed in 6-month-old rats between control and HS treatment. In aged animals, there was no difference in concentrations of muscle non-heme iron between cohorts of HS, 7 days and 14 days of re-loading.

Since HS affects iron and muscle weight in opposite manners, the total amount of non-heme iron in whole gastrocnemius muscle was calculated by multiplying non-heme iron concentration (μg/g) with the average muscle weight of left and right gastrocnemius muscles (g).

The total amount of non-heme iron in the gastrocnemius muscle of rats was significantly higher with age (age effect: $p<0.0001$; Fig. 1B). No significant treatment effect or interaction was observed for the total non-heme iron amount in the gastrocnemius muscle of rats.

3.3. Analysis of protein and gene expression of iron transporters and hemojuvelin (HJV) revealed specific alterations in the gastrocnemius muscle of old rats

Protein levels of HJV in the gastrocnemius muscle remained unchanged with age, HS or re-loading treatments (Fig. 2A). In support of this finding, gene expression results showed no significant difference in HJV mRNA levels between young and old control rats (Fig. 2B). However, 14 days of HS was associated with remarkably elevated HJV mRNA levels in both young and old rats ($p<0.05$). Seven and 14 days of re-loading following HS were associated with lower HJV mRNA levels in both young (HS vs. HS + 7, $p<0.001$; HS vs. HS + 14, $p<0.01$) and old rats (HS vs. HS + 7, ns; HS vs. HS + 14, $p<0.001$).

With regard to the primary cellular iron import protein TfR1, protein levels were significantly lower in old control rats as compared with their young counterparts (age effect: $p<0.0001$, Fig. 3A). TfR1 protein levels in the gastrocnemius muscle of old rats did not differ between groups. However, 7 and 14 days of recovery following HS were associated with elevated TfR1 levels in young rats (age × treatment interaction: $p<0.05$). There was a significant age-related decrease in TfR1 mRNA levels in the gastrocnemius muscle of rats (age, $p<0.0001$; Fig. 3B). Fourteen days of HS was associated with lower TfR1 mRNA levels in young, but not old rats in comparison with their age-matched controls.

Protein expression levels of Zip14 remained constant in control, HS, and HS plus 7 or 14 days of recovery in young rats (Fig. 3C). Fourteen days of HS was associated with elevated Zip14 levels in old rats in comparison with their non-HS controls. No difference was observed in Zip14 levels between HS and 7 days of recovery in both young and old rats. However, 14 days of recovery was associated with lower Zip14 levels in old animals in comparison with their age-matched 7- and 14-day HS cohorts. Zip14 mRNA levels remained unchanged with age and treatments (Fig. 3D).

Advanced age did not affect protein expression of DMT1 (Fig. 3E). However, HS was associated with significant higher protein levels of DMT1 in old animals, whereas no difference was detected in young rats (age × treatment interaction: $p<0.001$). This adaptation might at least in part account for the iron accumulation observed in old HS rats. Following 7 days of recovery, a marked higher DMT1 protein expression was observed in young rats, with a return to baseline levels at 14 days of recovery (Fig. 3E). In contrast, in old rats, the early recovery phase (7 days of re-loading) was accompanied by lower DMT1 protein and mRNA levels (with or without iron-response element, IRE and nonIRE) in comparison with their HS counterparts, which may be interpreted as a compensatory, yet imperfect, response to the significant higher muscle iron concentration. At 14 days of re-loading, difference between old HS and re-loading groups was observed in DMT1 mRNA, but not protein levels (Fig. 3F and G).

Moreover, we measured protein and mRNA levels of FPN in the gastrocnemius muscle of rats. The mRNA levels of FPN did not show any significant difference with age or HS (Fig. 3H). However, 7 and 14 days of re-loading after HS were significantly associated with reduced FPN mRNA abundance relative to age-matched HS rats, implying that less iron may be exported out of cells in aged skeletal muscle during recovery. Protein levels of FPN in rat gastrocnemius muscle were too low to be detected using immunoblot analysis (data not shown), indicating that the absence of a positive iron export mechanism in skeletal muscle may contribute to the non-heme iron accumulation observed in aged muscle.

3.4. HS was associated with higher levels of lipid peroxidation and nitrosative stress in old, but not young rats

Lipid peroxidation and nitrosative stress, determined as HNE-modified proteins and 3-nitrotyrosine levels, respectively, were measured in the gastrocnemius muscle of rats via dot blot analysis (Fig. 4). There was no difference observed in these markers between groups in young rats. In contrast, HS was associated with significantly elevated HNE protein adducts in old rats ($p<0.01$) in comparison

Table 2
Effects of aging, hindlimb suspension and re-loading on body weight (BW), gastrocnemius muscle wet weight (MW) and gastrocnemius muscle weight to body weight ratio (MW/BW) in Fischer344 × Brown Norway rats at 6 and 32 months of age.

Age	6-month				32-month			
Treatment	Control	HS	HS + 7-day	HS + 14-day	Control	HS	HS + 7-day	HS + 14-day
BW (g)	416 ± 10^{b}	325 ± 8^{a}	340 ± 10^{a}	355 ± 11^{a}	580 ± 19^{c}	463 ± 16^{b}	437 ± 6^{b}	450 ± 9^{b}
MW (g)	2.16 ± 0.05^{e}	1.42 ± 0.03^{b}	1.57 ± 0.05^{c}	1.82 ± 0.06^{d}	1.58 ± 0.04^{bc}	1.04 ± 0.03^{a}	1.12 ± 0.03^{a}	1.18 ± 0.08^{a}
MW/BW (mg/g)	5.11 ± 0.04^{e}	4.40 ± 0.05^{c}	4.67 ± 0.05^{d}	5.10 ± 0.03^{e}	2.75 ± 0.11^{b}	2.25 ± 0.06^{a}	2.65 ± 0.04^{b}	2.62 ± 0.18^{b}

Values are means ± SEM (n = 8). ^{a,b,c,d,e}Different letters are significantly different from each other ($p<0.05$ by Tukey's Multiple Comparison Test). The muscle weight is reported as the average weight of muscles from two legs. Control, non-suspended control; HS, 14 days of HS; HS + 7, 14 days of HS followed by 7 days of ambulatory re-loading; HS + 14, 14 days of HS followed by 14 days of ambulatory re-loading.

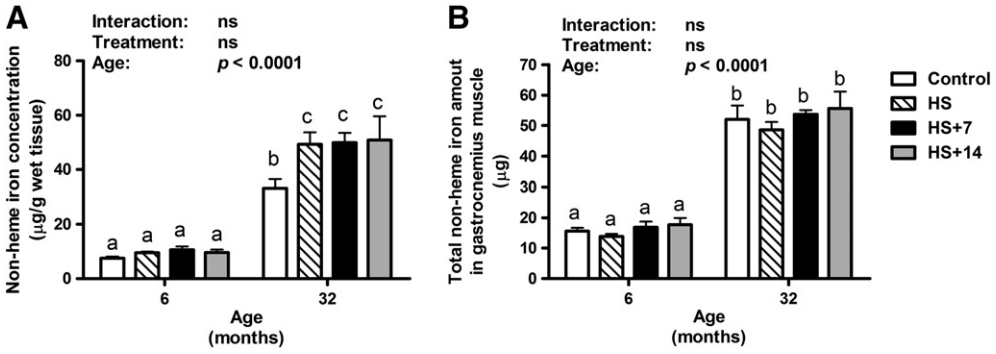

Fig. 1. Changes in non-heme iron levels (μg/g wet tissue) and total non-heme iron amounts (μg/muscle) in the gastrocnemius muscle of young and old rats with HS and re-loading treatments. (A) HS was associated with higher non-heme iron concentration in the gastrocnemius muscle of old ($p<0.05$), but not young rats. (B) Total amounts of non-heme iron were significantly higher in the gastrocnemius muscle of old rats (age effect: $p<0.0001$). However, neither HS nor re-loading following HS affected non-heme iron amount in the gastrocnemius muscle for both young and old rats, indicating that disuse-induced muscle loss in aged animals contributes to non-heme iron accumulation. Values are means ± SEM (n = 7–8). [a,b,c]Different letters are significantly different from each other ($p<0.05$). Graph bar legends: Control, non-suspended control; HS, 14 days of HS; HS + 7, 14 days of HS followed by 7 days of ambulatory re-loading; HS + 14, 14 days of HS followed by 14 days of ambulatory re-loading.

with their age-matched controls (Fig. 4A). Advanced age was associated with elevated nitrotyrosine levels (age effect: $p<0.0001$; Fig. 4B), with no difference with HS or re-loading treatments within each age cohort.

3.5. The age-associated increase in RNA, but not DNA, oxidation is exacerbated by HS

A significant higher level of RNA oxidation in the gastrocnemius muscle of old rats was detected in comparison with that in young controls (age effect: $p<0.001$, Fig. 4C). RNA oxidation levels remained fairly constant with HS and re-loading treatments in young rats. In contrast, HS was associated with much higher levels of RNA oxidative damage relative to controls in the gastrocnemius muscle of aged animals. A significant lower level of RNA oxidation was observed in 7 days of re-loading, but not 14 days of re-loading treatment between old HS and re-loading rats. In agreement with our previous findings (Hofer et al., 2008b), the extent of DNA oxidation was unaffected by age or HS (Fig. 4D). Furthermore, significant difference in DNA oxidative damage was not detected during re-loading within each age cohort.

4. Discussion

Sarcopenia, defined as the age-related degenerative loss of muscle mass, strength and function, is a serious health concern that contributes to disability, frailty and mortality in the elderly. The molecular mechanisms that contribute to sarcopenia are not fully understood. Recent advances in cellular and molecular biology have begun to unravel the complexity of the age-associated muscle atrophy, providing insights into the mechanisms behind the clinical manifestations. Recently, the role of iron in the pathogenesis of sarcopenia has attracted intense attention with respect to its potential as a mediator in oxidative stress pathways (Altun et al., 2007; Seo et al., 2008; Xu et al., 2008; Jung et al., 2008; Hofer et al., 2008b).

In agreement with previous findings from our group (Hofer et al., 2008b), advanced age was associated with higher levels of muscle non-heme iron, which were further elevated by disuse-induced atrophy. Since HS affects iron and muscle weight in opposite manners, the total amount of non-heme iron was calculated by multiplying non-heme iron concentration (μg/g) with the average muscle weight of left and right gastrocnemius muscles (g). The total amount of non-heme iron in the gastrocnemius muscle did not show any difference between groups within each age cohort, suggesting that advanced age is associated with non-heme iron accumulation in skeletal muscles and that muscle loss induced by HS contributes to remarkably high concentrations of non-heme iron in old rats. Although HS leads to muscle loss in both young and old rats, changes in the muscle weights of young rats did not result in significant changes in non-heme iron concentrations because of their relatively low non-heme iron amounts. However, slight loss in the muscle weight of old rats could lead to significant non-heme iron accumulation due to their significant high non-heme iron amounts in gastrocnemius muscles.

Mutations in the HJV gene cause juvenile hemochromatosis, characterized by hepcidin deficiency and severe iron overload (Papanikolaou et al., 2004). Disruption of the gene in the mouse results in increased iron deposition in liver, pancreas, and heart and decreased iron levels in tissue macrophages (Huang et al., 2005; Silvestri et al., 2007). A recent study by Chen et al. employing HJV conditional knockout mice has shown that HJV in skeletal muscle is dispensable

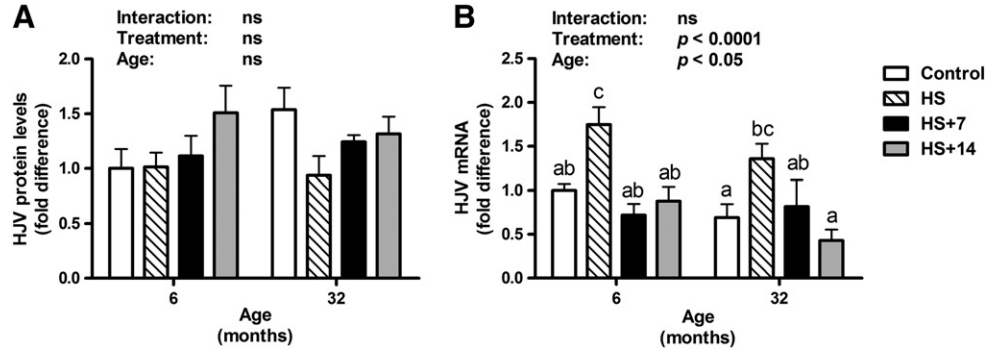

Fig. 2. Protein and gene expression of hemojuvelin (HJV) in the gastrocnemius muscle of young and old rats in control, HS, HS + 7 and HS + 14 groups. (A) The protein expression levels of HJV were unchanged with age and treatments. (B) HJV mRNA levels significantly elevated by HS in gastrocnemius muscle of both young and old rats, which subsequently mitigated by re-loading. Values are means ± SEM (n = 7–8). [a,b,c]Different letters are significantly different from each other ($p<0.05$). Graph bar legends: Control, non-suspended control; HS, 14 days of HS; HS + 7, 14 days of HS followed by 7 days of ambulatory re-loading; HS + 14, 14 days of HS followed by 14 days of ambulatory re-loading.

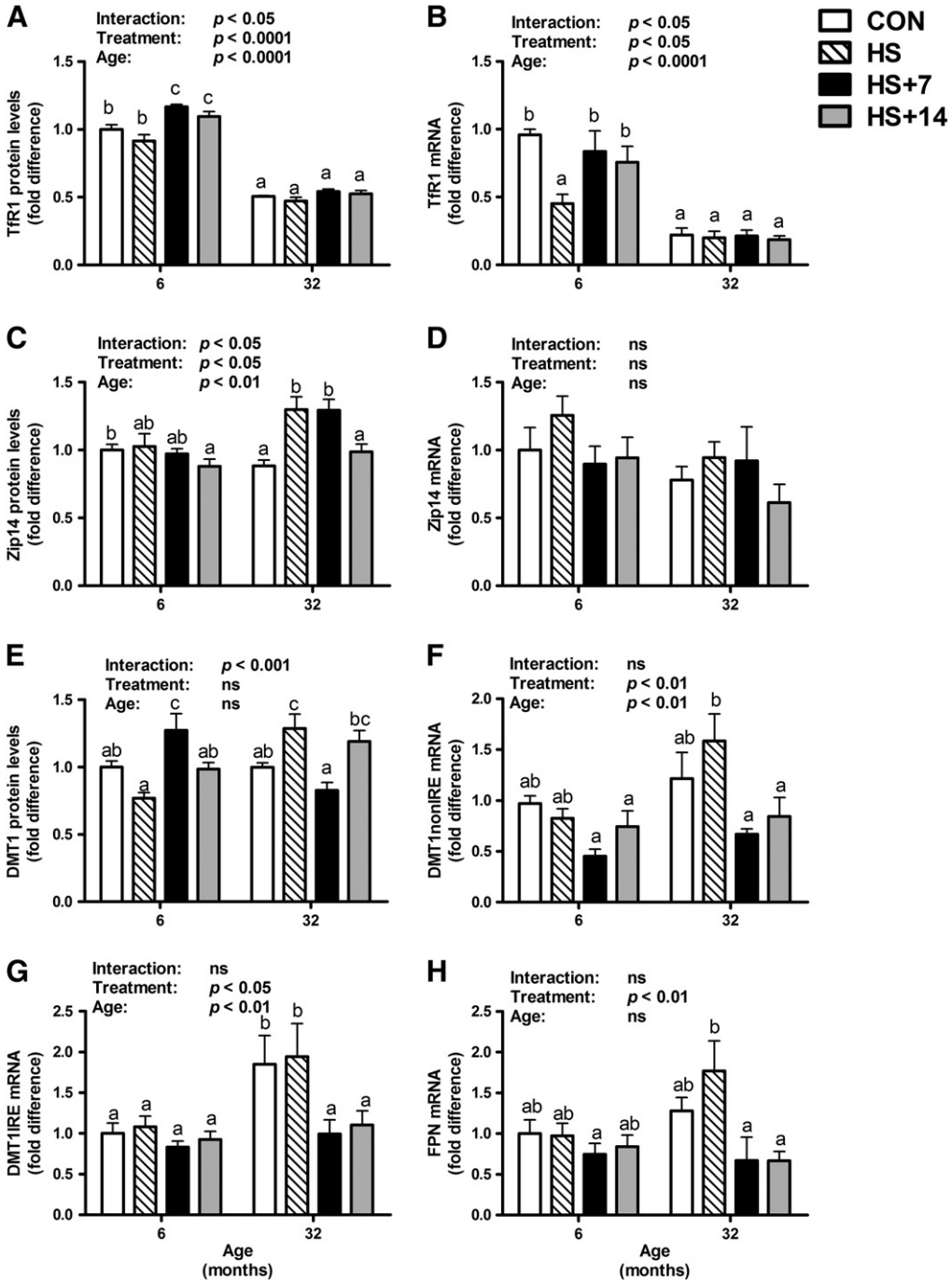

Fig. 3. Protein and gene expression levels of key iron transport proteins in the gastrocnemius muscle of young and old rats in control, HS, HS + 7 and HS + 14 groups. There was a significant age-related decrease in TfR1 protein (A) and gene expression (B) levels in gastrocnemius muscle ($p<0.0001$). Post hoc analysis showed that re-loading following HS was associated with higher TfR1 protein levels in the gastrocnemius muscle of young rats, whereas TfR1 protein and mRNA levels did not differ between groups in old rats. Significant age, treatment and interaction effects have been observed in Zip14 protein levels (C), though mRNA levels (D) were fairly constant. (E) HS was associated with higher DMT1 protein levels in the gastrocnemius muscle of aged, but not young rats. Moreover, the mRNA levels of DMT1 nonIRE (F) and IRE (G) in the gastrocnemius muscle of young and old rats were determined. With respect to the only known iron export protein in mammals, the mRNA levels of FPN (H) didn't change with age or HS in gastrocnemius muscles. However, 7 and 14 days of re-loading after HS in old rats was associated with lower FPN mRNA levels in comparison with their age-matched HS animals. Values are means ± SEM (n = 7–8). [a,b,c]Different letters are significantly different from each other ($p<0.05$). Graph bar legends: Control, non-suspended control; HS, 14 days of HS; HS + 7, 14 days of HS followed by 7 days of ambulatory re-loading; HS + 14, 14 days of HS followed by 14 days of ambulatory re-loading.

for systemic iron homeostasis (Chen et al., 2011). Our results suggest that HJV in skeletal muscle may also be dispensable for iron homeostasis in skeletal muscle.

In the present study, we also determined the expression levels of key membrane iron transport proteins and their mRNA abundance to investigate age-related changes of iron metabolism in skeletal muscle with unloading as well as re-loading. The TfR1-mediated iron import pathway is the primary route of cellular iron acquisition and its expression is commensurate to cellular iron uptake (Hofer et al., 2008a). In agreement with findings from Jung et al. (2008), both TfR1 protein and mRNA levels were remarkably lower in old animals, indicating that TfR1-mediated cellular iron acquisition

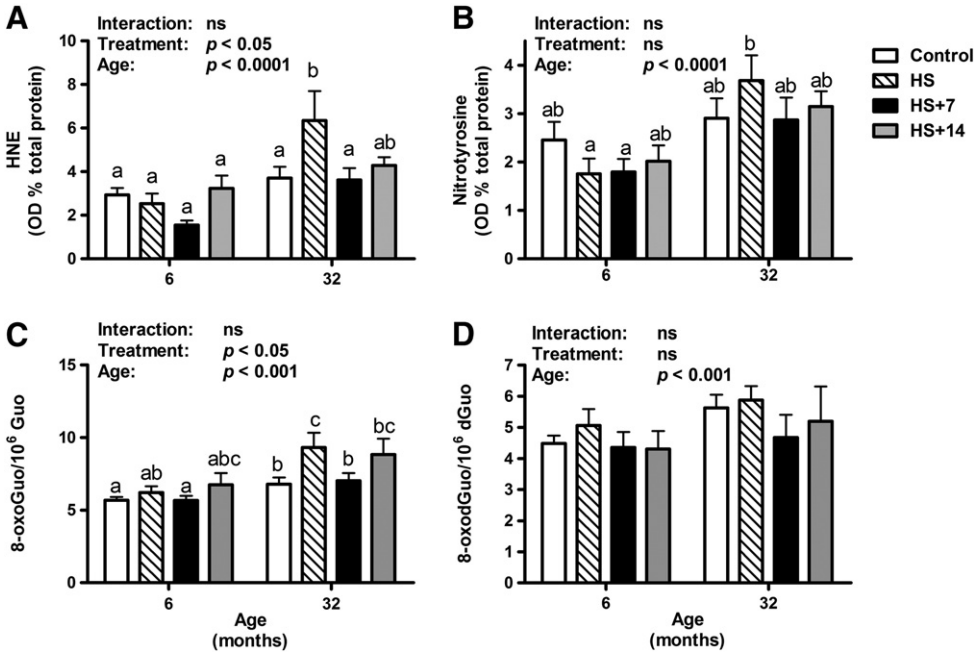

Fig. 4. Oxidative damage in the gastrocnemius muscle of rats as determined by dot blot analysis and HPLC-ECD. (A) HS was associated with higher HNE-modified protein levels ($p<0.01$) in the gastrocnemius muscle of old, but not young rats. Seven days of re-loading following HS was associated with lower levels of HNE-modified proteins in old HS rats ($p<0.01$). (B) There was a significant increase in nitrotyrosine levels with age ($p<0.0001$). (C–D) Oxidative damage to RNA and DNA in gastrocnemius muscle was assessed as their oxidation products 8-oxo-7,8-dihydroguanosine (8-oxoGuo) and 8-oxo-7,8-dihydro-2′-oxyguanosine (8-oxodGuo), respectively. (C) Greater RNA oxidation level in gastrocnemius muscle was associated with age (age, $p<0.001$). (D) The DNA oxidation levels did not change significantly over the course of aging and treatments. Values are means ± SEM (n = 7–8). [a,b,c]Different letters are significantly different from each other ($p<0.05$). Graph bar legends: Control, non-suspended control; HS, 14 days of HS; HS + 7, 14 days of HS followed by 7 days of ambulatory re-loading; HS + 14, 14 days of HS followed by 14 days of ambulatory re-loading.

decreases with age in skeletal muscles. Age-related decrease of TfR1 may be interpreted as a compensatory response to high iron concentrations in the gastrocnemius muscle of aged animals. Other cellular iron import proteins, including DMT1 and Zip14, did not show any difference between groups in young animals, but remarkably higher levels were observed in old HS animals, suggesting that they may play an important role in HS-induced iron accumulation in aged animals.

Since HJV has been shown to modulate the expression of hepcidin, the central regulator of whole body iron homeostasis (Nemeth and Ganz, 2009; Ganz and Nemeth, 2011), we also determined HJV protein and mRNA levels. Although mRNA levels of HJV in the gastrocnemius muscle of both young and old rats were higher in HS treatment, the protein expression levels of HJV remained fairly constant between young and old rats as well as treatment groups within each age cohort, suggesting that HJV plays a very minor role in modulating iron metabolism in the skeletal muscle of rats. Indeed, Zhang et al. (2007) reported that muscular HJV levels were independent of body iron status.

Moreover, we measured both FPN protein and mRNA levels in the gastrocnemius muscle of rats. FPN mRNA abundance did not show any difference between young and old rats or control and HS treatment. However, 7 and 14 days of re-loading after HS were associated with lower FPN mRNA levels in old rats in comparison with their age-matched HS animals, which may suggest that iron export is compromised following HS in old rats. Moreover, protein levels of FPN (the only known iron exporter in mammals) in rat gastrocnemius muscle were too low to be detected using immunoblot analysis, indicating that iron export in the gastrocnemius muscle of rats is likely negligible, contributing to age-related non-heme iron accumulation. As a whole, our data suggest that muscular iron import is greater than iron export, which may lead to non-heme iron accumulation in aged muscles.

In agreement with our previous study (Hofer et al., 2008b), RNA oxidative damage was elevated in muscles of aged animals, in particular after a period of disuse. Seven days of re-loading was associated with lower levels of RNA oxidation relative to HS in aged rats, whereas RNA oxidation levels did not show any difference between HS and 14 days of re-loading, suggesting that HS is associated with persistent muscle oxidative damage in aged animals. In contrast, levels of DNA oxidation remained fairly constant in the gastrocnemius muscle of both young and old rats as well as in all treatment groups. This observation complements our previous investigations (Hofer et al., 2006, 2008b; Seo et al., 2006, 2008; Xu et al., 2010a) confirming that that RNA is more susceptible to oxidative damage than DNA in aged skeletal muscle likely due to its widespread cytosolic distribution and the lack of repair and turnover mechanisms. Furthermore, we found that changes in HNE protein adducts and 3-nitrotyrosine levels in the gastrocnemius muscle of rats were analogous to those of RNA damage, indicating that HS in advanced age induces extensive oxidative damage which persists over the long-term, possibly impairing recovery from muscle atrophy.

We further examined specific correlations between non-heme iron levels (amount or concentration) and muscle mass, as well as between non-heme iron levels and oxidative damage markers (Table 3).

Table 3
Correlations of iron levels with muscle weights (MW), muscle weight-to-body weight ratio (MW/BW) and oxidative markers.

Correlation	p Value	Pearson r	R squared
Non-heme iron concentration vs. MW	<0.0001	−0.7742	0.5994
Total iron amount vs MW	<0.0001	−0.6389	0.4082
Non-heme iron concentration vs. MW/BW	<0.0001	−0.8756	0.7666
Total iron amount vs. MW/BW	<0.0001	−0.8851	0.7833
Non-heme iron concentration vs. HNE	<0.0001	0.5041	0.2541
Total iron amount vs. HNE	<0.001	0.4352	0.1894
Non-heme iron concentration vs. nitrotyrosine	<0.01	0.3996	0.1597
Total iron amount vs. nitrotyrosine	<0.01	0.3533	0.1249
Non-heme iron concentration vs. RNA oxidation	<0.0001	0.5391	0.2907
Total iron amount vs. RNA oxidation	<0.001	0.4616	0.2131

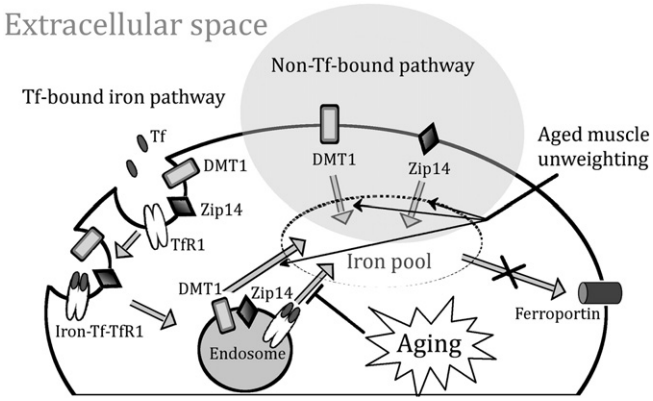

Fig. 5. Changes of iron homeostasis with aging and muscle unweighting in the skeletal muscle of Fischer344×Brown Norway rats. Muscle iron import via TfR1 is lower in old rats, which may represent a compensatory mechanism aimed at countering excessive iron accumulation. However, age-related iron accumulation may be due to the extremely low expression of FPN in the skeletal muscle, which might result in an ineffective iron export with age. DMT1- and Zip14-mediated iron uptake during HS may be at least partly responsible for non-heme iron overload in the atrophying muscle of aged animals.

There was a significant negative correlation between non-heme iron levels and muscle mass ($p<0.0001$). With respect to oxidative damage, iron levels (amount or concentration) correlated with HNE (vs. iron amount, $r=0.4352$, $p<0.001$; vs. iron concentration, $r=0.5041$, $p<0.0001$), nitrotyrosine (vs. iron amount, $r=0.3533$, $p<0.01$; vs. iron concentration, $r=0.3996$, $p<0.01$) and oxidized RNA (vs. iron amount, $r=0.4616$, $p<0.001$; vs. iron concentration, $r=0.5391$, $p<0.0001$) levels. The negative relationship between iron and muscle mass implies that higher iron content is associated with lower muscle mass. Moreover, the positive correlations between iron levels and oxidative damage markers support the notion that higher non-heme levels may be linked to a greater release of free iron, which has a strong catalytic potential to generate cellular damage (Table 3).

In our previous study, representative histology results have shown that muscle fibers with iron overload were associated with cell death and atrophy (Hofer et al., 2008b). An additional study investigating the physical performance in iron-overloaded animals by Reardon and Allen has demonstrated that iron has the potential to induce significant changes in muscle function and contribute to weakness, fatigue and reduced exercise capacity (Reardon and Allen, 2009). Moreover, the observation that removing iron using an iron chelator, deferoxamine, ameliorated immobilization-induced muscle atrophy suggests that iron accumulation occurring with disuse is not actually part of the normal physiological mechanism by which atrophy occurs, but a pathological event contributing to muscle atrophy (Kondo et al., 1992).

5. Conclusions

The current study shows for the first time that advanced age is associated with specific alterations in muscle iron handling. Acute muscle atrophy induced by HS is associated with further perturbations in iron homeostasis in aged muscles. The persistence of elevated iron levels during re-loading is linked with extensive oxidative damage to muscle macromolecules, which may partly explain the impaired recovery from atrophy experienced by old rats. Muscle iron import via TfR1 is lower in old rats, which may represent a compensatory mechanism aimed at countering excessive iron accumulation (Fig. 5). However, DMT1- and Zip14-mediated iron uptake during HS may be at least partly responsible for non-heme iron overload in the atrophying muscle of aged animals (Fig. 5). This condition may be further aggravated by the extremely low expression of FPN in skeletal muscle, which might result in an ineffective iron export in the presence of iron overload. Future research is warranted to determine whether iron chelation/removal protects against age-related muscle atrophy, especially during periods of prolonged disuse.

6. Limitations of the study

One limitation of the current study is that mixed-fiber gastrocnemius muscles were used. Thus, the association of a particular sub-population of fibers (Type I or Type II fibers) with iron accumulation in aging muscle could not be established. In addition, the accumulation of iron in skeletal muscles could be one of the potential contributors to accelerate the denervation of aged myofibers, which may be the primary cause of fiber atrophy in aging muscle (Rowan et al., 2011). Additional studies are warranted to further critically assess iron levels and their impact on muscle denervation and atrophy in different sub-populations of fibers.

Acknowledgments

This research was supported by grants to C.L. (NIH AG17994), E.E.D.V. (NIH AG028925), M.D.K. (NIH DK080706), the University of Florida Institute on Aging and Claude D. Pepper Older Americans Independence Center (1 P30AG028740) and fellowship award from the American Heart Association to J.X. (09POST2060112). We would like to thank Dr. Philippe Gros (McGill University, Quebec, CA) for providing anti-DMT1 antibody and Dr. An-Sheng Zhang (Oregon Health and Science University, Portland, OR) for providing anti-hemojuvelin antibody.

References

Altun, M., Edstrom, E., Spooner, E., Flores-Moralez, A., Bergman, E., Tollet-Egnell, P., Norstedt, G., Kessler, B.M., Ulfhake, B., 2007. Iron load and redox stress in skeletal muscle of aged rats. Muscle Nerve 36, 223–233.
Bian, K., Gao, Z., Weisbrodt, N., Murad, F., 2003. The nature of heme/iron-induced protein tyrosine nitration. Proc. Natl. Acad. Sci. U. S. A. 100, 5712–5717.
Bradford, M.M., 1976. A rapid and sensitive method for the quantitation of microgram quantities of protein utilizing the principle of protein–dye binding. Anal. Biochem. 72, 248–254.
Chen, W., Huang, F.W., de Renshaw, T.B., Andrews, N.C., 2011. Skeletal muscle hemojuvelin is dispensable for systemic iron homeostasis. Blood 117, 6319–6325.
Chua, A.C., Graham, R.M., Trinder, D., Olynyk, J.K., 2007. The regulation of cellular iron metabolism. Crit. Rev. Clin. Lab. Sci. 44, 413–459.
Donovan, A., Lima, C.A., Pinkus, J.L., Pinkus, G.S., Zon, L.I., Robine, S., Andrews, N.C., 2005. The iron exporter ferroportin/Slc40a1 is essential for iron homeostasis. Cell Metab. 1, 191–200.
Dunn, L.L., Rahmanto, Y.S., Richardson, D.R., 2007. Iron uptake and metabolism in the new millennium. Trends Cell Biol. 17, 93–100.
Gallegly, J.C., Turesky, N.A., Strotman, B.A., Gurley, C.M., Peterson, C.A., Dupont-Versteegden, E.E., 2004. Satellite cell regulation of muscle mass is altered at old age. J. Appl. Physiol. 97, 1082–1090.

Ganz, T., Nemeth, E., 2011. Hepcidin and disorders of iron metabolism. Annu. Rev. Med. 62, 347–360.
Hansen, S.L., Ashwell, M.S., Moeser, A.J., Fry, R.S., Knutson, M.D., Spears, J.W., 2010. High dietary iron reduces transporters involved in iron and manganese metabolism and increases intestinal permeability in calves. J. Dairy Sci. 93, 656–665.
Hider, R.C., Zhou, T., 2005. The design of orally active iron chelators. Ann. N. Y. Acad. Sci. 1054, 141–154.
Hofer, T., Seo, A.Y., Prudencio, M., Leeuwenburgh, C., 2006. A method to determine RNA and DNA oxidation simultaneously by HPLC-ECD: greater RNA than DNA oxidation in rat liver after doxorubicin administration. Biol. Chem. 387, 103–111.
Hofer, T., Marzetti, E., Seo, A.Y., Xu, J., Knutson, M.D., Leeuwenburgh, C., 2008a. Mechanisms of iron regulation and oxidative stress in sarcopenia and neurodegenerative diseases. In: Gutierrez-Merino, C., Leeuwenburgh, C. (Eds.), Free Radicals in Biology and Medicine. Research Signpost, Kerala, pp. 1–22.
Hofer, T., Marzetti, E., Xu, J., Seo, A.Y., Gulec, S., Knutson, M.D., Leeuwenburgh, C., Dupont-Versteegden, E.E., 2008b. Increased iron content and RNA oxidative damage in skeletal muscle with aging and disuse atrophy. Exp. Gerontol. 43, 563–570.
Huang, F.W., Pinkus, J.L., Pinkus, G.S., Fleming, M.D., Andrews, N.C., 2005. A mouse model of juvenile hemochromatosis. J. Clin. Invest. 115, 2187–2191.
Jung, S.H., DeRuisseau, L.R., Kavazis, A.N., Deruisseau, K.C., 2008. Plantaris muscle of aged rats demonstrates iron accumulation and altered expression of iron regulation proteins. Exp. Physiol. 93, 407–414.
Knutson, M.D., Oukka, M., Koss, L.M., Aydemir, F., Wessling-Resnick, M., 2005. Iron release from macrophages after erythrophagocytosis is up-regulated by ferroportin 1 overexpression and down-regulated by hepcidin. Proc. Natl. Acad. Sci. U. S. A. 102, 1324–1328.
Kohgo, Y., Ikuta, K., Ohtake, T., Torimoto, Y., Kato, J., 2008. Body iron metabolism and pathophysiology of iron overload. Int. J. Hematol. 88, 7–15.
Kondo, H., Miura, M., Kodama, J., Ahmed, S.M., Itokawa, Y., 1992. Role of iron in oxidative stress in skeletal muscle atrophied by immobilization. Pflugers Arch. 421, 295–297.
Leverence, R., Mason, A.B., Kaltashov, I.A., 2010. Noncanonical interactions between serum transferrin and transferrin receptor evaluated with electrospray ionization mass spectrometry. Proc. Natl. Acad. Sci. U. S. A. 107, 8123–8128.
Lill, R., Muhlenhoff, U., 2006. Iron-sulfur protein biogenesis in eukaryotes: components and mechanisms. Annu. Rev. Cell Dev. Biol. 22, 457–486.
Liuzzi, J.P., Aydemir, F., Nam, H., Knutson, M.D., Cousins, R.J., 2006. Zip14 (Slc39a14) mediates non-transferrin-bound iron uptake into cells. Proc. Natl. Acad. Sci. U. S. A. 103, 13612–13617.
Livak, K.J., Schmittgen, T.D., 2001. Analysis of relative gene expression data using real-time quantitative PCR and the 2(−Delta Delta C(T)) method. Methods 25, 402–408.
Marzetti, E., Groban, L., Wohlgemuth, S.E., Lees, H.A., Lin, M., Jobe, H., Giovannini, S., Leeuwenburgh, C., Carter, C.S., 2008a. Effects of short-term GH supplementation and treadmill exercise training on physical performance and skeletal muscle apoptosis in old rats. Am. J. Physiol. Regul. Integr. Comp. Physiol. 294, R558–R567.
Marzetti, E., Wohlgemuth, S.E., Lees, H.A., Chung, H.Y., Giovannini, S., Leeuwenburgh, C., 2008b. Age-related activation of mitochondrial caspase-independent apoptotic signaling in rat gastrocnemius muscle. Mech. Ageing Dev. 129, 542–549.
Marzetti, E., Carter, C.S., Wohlgemuth, S.E., Lees, H.A., Giovannini, S., Anderson, B., Quinn, L.S., Leeuwenburgh, C., 2009. Changes in IL-15 expression and death-receptor apoptotic signaling in rat gastrocnemius muscle with aging and life-long calorie restriction. Mech. Ageing Dev. 130, 272–280.
Nemeth, E., Ganz, T., 2009. The role of hepcidin in iron metabolism. Acta Haematol. 122, 78–86.
Papanikolaou, G., Samuels, M.E., Ludwig, E.H., MacDonald, M.L., Franchini, P.L., Dube, M.P., Andres, L., MacFarlane, J., Sakellaropoulos, N., Politou, M., Nemeth, E., Thompson, J., Risler, J.K., Zaborowska, C., Babakaiff, R., Radomski, C.C., Pape, T.D., Davidas, O., Christakis, J., Brissot, P., Lockitch, G., Ganz, T., Hayden, M.R., Goldberg, Y.P., 2004. Mutations in HFE2 cause iron overload in chromosome 1q-linked juvenile hemochromatosis. Nat. Genet. 36, 77–82.
Reardon, T.F., Allen, D.G., 2009. Iron injections in mice increase skeletal muscle iron content, induce oxidative stress and reduce exercise performance. Exp. Physiol. 94, 720–730.
Rebouche, C.J., Wilcox, C.L., Widness, J.A., 2004. Microanalysis of non-heme iron in animal tissues. J. Biochem. Biophys. Methods 58, 239–251.
Rowan, S.L., Purves-Smith, F.M., Solbak, N.M., Hepple, R.T., 2011. Accumulation of severely atrophic myofibers marks the acceleration of sarcopenia in slow and fast twitch muscles. Exp. Gerontol. 46, 660–669.
Seo, A.Y., Hofer, T., Sung, B., Judge, S., Chung, H.Y., Leeuwenburgh, C., 2006. Hepatic oxidative stress during aging: effects of 8% long-term calorie restriction and life-long exercise. Antioxid. Redox Signal. 8, 529–538.
Seo, A.Y., Xu, J., Servais, S., Hofer, T., Marzetti, E., Wohlgemuth, S.E., Knutson, M.D., Chung, H.Y., Leeuwenburgh, C., 2008. Mitochondrial iron accumulation with age and functional consequences. Aging Cell 7, 706–716.
Silvestri, L., Pagani, A., Fazi, C., Gerardi, G., Levi, S., Arosio, P., Camaschella, C., 2007. Defective targeting of hemojuvelin to plasma membrane is a common pathogenetic mechanism in juvenile hemochromatosis. Blood 109, 4503–4510.
Wacker, W., Vallee, B., 1959. Nucleic acids and metals. J. Biol. Chem. 234, 3257–3262.
Xu, J., Knutson, M.D., Carter, C.S., Leeuwenburgh, C., 2008. Iron accumulation with age, oxidative stress and functional decline. PLoS One 3, e2865.
Xu, J., Marzetti, E., Seo, A.Y., Kim, J.S., Prolla, T.A., Leeuwenburgh, C., 2010a. The emerging role of iron dyshomeostasis in the mitochondrial decay of aging. Mech. Ageing Dev. 131, 487–493.
Xu, M., Kashanchi, F., Foster, A., Rotimi, J., Turner, W., Gordeuk, V.R., Nekhai, S., 2010b. Hepcidin induces HIV-1 transcription inhibited by ferroportin. Retrovirology 7, 104.
Zarzhevsky, N., Carmeli, E., Fuchs, D., Coleman, R., Stein, H., Reznick, A.Z., 2001. Recovery of muscles of old rats after hindlimb immobilisation by external fixation is impaired compared with those of young rats. Exp. Gerontol. 36, 125–140.
Zhang, A.S., Anderson, S.A., Meyers, K.R., Hernandez, C., Eisenstein, R.S., Enns, C.A., 2007. Evidence that inhibition of hemojuvelin shedding in response to iron is mediated through neogenin. J. Biol. Chem. 282, 12547–12556.
Zhang, A.S., Gao, J., Koeberl, D.D., Enns, C.A., 2010. The role of hepatocyte hemojuvelin in the regulation of bone morphogenic protein-6 and hepcidin expression in vivo. J. Biol. Chem. 285, 16416–16423.
Zhao, N., Gao, J., Enns, C.A., Knutson, M.D., 2010. ZRT/IRT-like protein 14 (ZIP14) promotes the cellular assimilation of iron from transferrin. J. Biol. Chem. 285, 32141–32150.